Available online at www.sciencedirect.com
ScienceDirect
Biochemical and Biophysical Research Communications 360 (2007) 464–469
BBRC
www.elsevier.com/locate/ybbrc

Endogenous metalloprotease solubilizes IL-13 receptor α2 in airway epithelial cells ☆

Mikiko Matsumura [a], Hiromasa Inoue [a,*], Takafumi Matsumoto [a], Takako Nakano [a], Satoru Fukuyama [a], Koichiro Matsumoto [a], Koichi Takayama [a], Makoto Saito [b], Koji Kawakami [c], Yoichi Nakanishi [a]

[a] *Research Institute for Diseases of the Chest, Graduate School of Medical Sciences, Kyushu University, 3-1-1 Maidashi, Higashi-ku, Fukuoka 812-8582, Japan*
[b] *Laboratory of Molecular Biology of Infectious Agents, Graduate School of Biomedical Sciences, Nagasaki University, 1-14 Bunkyo-machi, Nagasaki 852-8521, Japan*
[c] *Department of Pharmacoepidemiology, School of Medicine and Public Health, Kyoto University, Yoshida Konoecho, Sakyoku, Kyoto 606-8501, Japan*

Received 7 June 2007
Available online 19 June 2007

Abstract

IL-13 receptor α2 (IL-13Rα2) has been postulated to be a decoy receptor. The precise mechanisms for the generation of soluble IL-13Rα2 and the biological activity of the endogenous soluble form have not been reported. Hypothesizing that the soluble form of IL-13Rα2 is generated by proteolytic cleavage of membrane-bound receptors, we transfected human airway epithelial cells with adenoviral vectors encoding full-length IL-13Rα2. Eotaxin production from IL-13Rα2-transfected cells was suppressed, and soluble IL-13Rα2 in the supernatants was increased time-dependently after the transfection. The transfer of conditioned media from IL-13Rα2-transfected cells inhibited IL-13-induced eotaxin production and STAT6 phosphorylation in non-transfected cells. PMA enhanced the release of soluble IL-13Rα2, and metalloprotease inhibitors inhibited this release. These findings suggest that airway epithelial cells with upregulation of membrane-bound IL-13Rα2 secrete soluble IL-13Rα2 into its supernatant, causing the autocrine and paracrine downregulation of the IL-13/STAT6 signal. Metalloprotease(s) are responsible for the proteolytic cleavage of cell surface IL-13Rα2.

Keywords: Th2 cytokine; Soluble receptor; Protease; Phorbol 12-myristate 13-acetate

Interleukin (IL)-13, a type 2 helper T (Th2) cytokine, plays important role in asthma by enhancing the recruitment of eosinophils, stimulating IgE-producing B cells, and directly inducing airway hyperresponsiveness [1–3]. IL-13 mediates its effects via a complex receptor system including IL-4Rα, IL-13Rα1, and IL-13Rα2. IL-13 binds to the primary receptor IL-13Rα1 chain with low affinity [4,5]. However, with the IL-4Rα chain, IL-13Rα1 binds IL-13 with high affinity and results in the activation of the janus-activated kinase (JAK)-STAT pathway [6]. IL-13 also binds to a second receptor, IL-13Rα2, but with high affinity [7,8].

The IL-13Rα2 chain has not been shown to mediate signaling through the JAK-STAT pathway [9,10] because its short cytoplasmic region (17 amino acids in the human) does not contain an obvious signaling motif or JAK-STAT binding sequence [8]. IL-13Rα2 knockout mice showed enhanced IL-13 responses [11,12]; therefore, IL-13Rα2 has been postulated to be a decoy receptor. Recently, it has been demonstrated that IL-13-induced TGF-β1-mediated fibrosis depends on IL-13Rα2 signals through the AP-1 pathway, and IL-13Rα2 may also contribute to IL-13 responses [13].

☆ This work was supported in part by Grant-in-Aid for Scientific Research from the Japan Society for the Promotion of Science.
* Corresponding author. Fax: +81 92 642 5389.
E-mail address: inoue@kokyu.med.kyushu-u.ac.jp (H. Inoue).

0006-291X/$ - see front matter © 2007 Elsevier Inc. All rights reserved.
doi:10.1016/j.bbrc.2007.06.076

IL-13Rα2 has been shown to be predominantly an intracellular molecule mobilized to the cell surface from intracellular stores [14]. The extracellular domain of IL-13Rα2 could be cleaved. The overexpression of the IL-13Rα2 extracellular domain inhibits the biological activity of IL-13 [15]. The precise mechanism of the generation of soluble IL-13Rα2 is unclear, however, and the inhibitory action of the soluble form after the enhanced expression of the full-length IL-13Rα2 chain has not yet been reported.

Soluble cytokine receptors can be generated by several mechanisms, including the proteolytic cleavage of membrane-bound receptor proteins from the cell surface and alternative splicing of mRNA transcripts [16]. The release of the soluble proteins can be strongly stimulated by phorbol ester PMA, a potent activator of protein kinase C [17]. We examined whether the transfection with the full-length IL-13Rα2 chain to human airway epithelial cells increases the generation of soluble IL-13Rα2, and we studied the inhibitory effects of the soluble form on IL-13 response. We also stimulated the cells with PMA after full-length IL-13Rα2 transfection and examined the effect of protease inhibitors in order to characterize the release of soluble IL-13Rα2.

Materials and methods

Cell culture. BEAS-2B cells, a human airway epithelial cell line transformed with the SV40 virus, were cultured in DMEM/F-12 medium with 10% FBS, penicillin, and streptomycin.

Adenovirus transfection and stimulation. A replication-defective ΔE1ΔE3 adenoviral vector expressing the IL-13Rα2 chain gene under the CMV promoter (Ad-IL-13Rα2) was constructed as described previously [18]. Another replication-defective adenoviral vector expressing the β-galactosidase gene (Ad-LacZ) was constructed in the same way and utilized as an adenoviral infection control.

BEAS-2B cells were seeded in 6-well tissue culture plates until subconfluence and infected with Ad-LacZ or Ad-IL-13Rα2 diffused in DMEM/F12 medium with 2% FBS for 2 h. Cells were washed and cultured in DMEM/F12 medium with 10% FBS as indicated in each experiment. Then, after 2 h of serum starvation, the cells were stimulated with human rIL-13.

Supernatants were collected at 72 h after transfection and concentrated to about one-seventh of the original volume by centrifugal filtration through the MW 10,000 cutoff membrane (Millipore, Bedford, MA). Other cells were stimulated with human rIL-13 dissolved in concentrated medium.

To remove remaining IL-13Rα2 vectors in supernatants, trypsin was used 2 h after transfection, and the cells were re-seeded in culture dishes.

Measurement of eotaxin and soluble IL-13Rα2. The concentrations of eotaxin were measured in the cell supernatant fluids from BEAS-2B using ELISA [19]. The minimum concentration detected by this method was 5 pg/ml. Quantification of human-soluble IL-13Rα2 expression was done with ELISA (R&D Systems).

Analysis of effect of PMA on release of soluble IL-13Rα2. After 2 h of serum starvation, cells were treated with stimuli as indicated in each experiment. For inhibitor studies, serum-starved cells were pretreated with inhibitors for 30 min before exposure to stimuli. In studies of PMA, cells were treated with PMA (10 ng/ml) for 2 h. Supernatants were collected for the measurement of soluble IL-13Rα2 by ELISA.

Western blotting analysis. After cytokine treatment, protein extracts from the cells were prepared with lysis buffer. Immunoblotting was performed using anti-phospho STAT6, or anti-STAT6 antibodies, as described [19,20].

RT-PCR analysis. Total RNA was isolated, and reverse transcription (RT)-polymerase chain reaction (PCR) was performed on 1.0 μg total RNA. An oligo (dT) primer was used for RT, and cDNA was amplified by PCR using specific primers. The following primer pairs specific for IL-13Rα2 and for β-actin were used: 5′-AATGGCTTTCGTTTGCTTGG-3′ and 5′-ACGCAATCCATATCCTGAAC-3′; and 5′-TCCTGTGGCA TCCATGAAACT-3′ and 5′-GAAGCACTTGCGGTGCACGAT-3′, respectively. Amplification was performed as previously reported [19].

Data analysis. Values are expressed as means ± SEM. Differences between groups were analyzed by ANOVA, and the significance of differences between values was assessed with the Bonferroni correction. A P value below 0.05 was considered significant.

Results

IL-13Rα2 gene induction in airway epithelial cells and secretion of soluble L-13Rα2

IL-13Rα2 mRNA levels were barely detectable in BEAS-2B cells. To establish airway epithelial cells with a high expression of IL-13Rα2, BEAS-2B cells were transfected with a full-length IL-13Rα2 using Ad-IL-13Rα2. Ad-IL-13Rα2 transfection, but not Ad-LacZ, induced IL-13 Rα2 mRNA in a multiplicity of infection (moi)-dependent manners (Fig. 1A). Maximal induction of IL-13Rα2 was observed at 30-moi transfection of Ad-IL-13Rα2. We also analyzed the time kinetics of IL-13Rα2 mRNA expression. The high levels of IL-13Rα2 mRNA expression were sustained for 24–48 h after transfection in BEAS-2B cells (Fig. 1B). To confirm the IL-13Rα2 protein on the surface of IL-13Rα2-transfected cells, flow cytometric analysis was performed using the FITC-conjugated antibody against the human IL-13Rα2 chain. IL-13Rα2 expression was detected at the surface of BEAB-2B cells transfected with Ad-IL-13Rα2 but not with Ad-LacZ (data not shown).

IL-13 induces eotaxin in the airways STAT6-dependently [21,22], and IL-13Rα2 has been reported to limit IL-13-mediated responses through the JAK/STAT6 pathway as a "decoy" receptor [9,12,23]. To confirm the function of overexpressed membrane IL-13Rα2 in airway epithelial cells, we analyzed eotaxin production and STAT6 phosphorylation induced by IL-13. Transfection of Ad-IL-13Rα2, but not of Ad-LacZ, inhibited IL-13-induced STAT6 activation (data not shown) and eotaxin production in BEAS-2B cells (Fig. 1C), suggesting that the overexpression of IL-13Rα2 on the surface of airway epithelial cells leads to the inhibition of STAT6-dependent signals in the cells.

To test whether a soluble form of IL-13Rα2 is secreted after IL-13Rα2 transduction, BEAS-2B cells were transduced with 30-moi Ad-IL-13Rα2, and the concentration of soluble IL-13Rα2 in the supernatant of the cells was measured by ELISA. There was a time-dependent increase in the level of soluble IL-13Rα2 in the conditioned media, indicating the spontaneous release of soluble IL-13Rα2

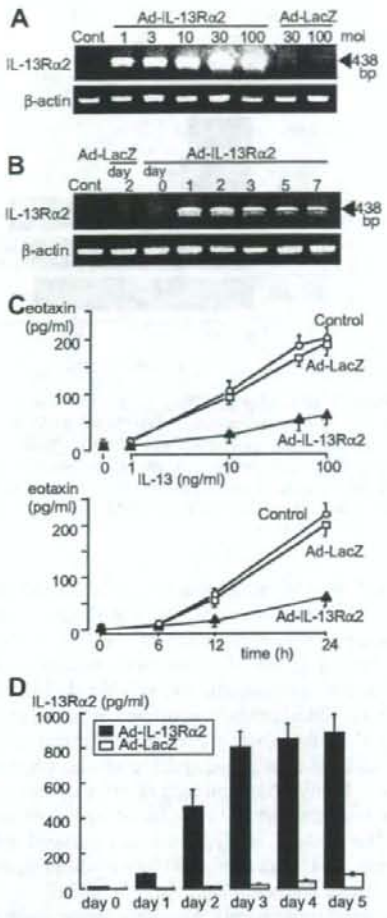

Fig. 1. Effects of transfection with a full-length IL-13Rα2 using adenoviral vectors (Ad-IL-13Rα2) on IL-13Rα2 expression, IL-13-induced eotaxin production, and soluble IL-13Rα2 secretion from airway epithelial cells. (A) BEAS-2B cells were transfected with Ad-IL-13Rα2 or the control adenoviral vector (Ad-LacZ) at the indicated multiplicity of infection (moi). The total RNA was isolated from the cells 3 days after the transfection or from untransfected cells (Cont), and IL-13Rα2 levels were amplified by RT-PCR. RT-PCR products for β-actin are shown for comparison. Amplified DNA was separated by electrophoresis on an agarose gel containing ethidium bromide, illuminated with ultraviolet light, and photographed. (B) BEAS-2B cells were transfected with Ad-IL-13Rα2 or Ad-LacZ (30 moi). On the indicated days after transfection, total RNA was isolated from the cells, and IL-13Rα2 levels were amplified by RT-PCR. (C) Dose-dependent and time-dependent eotaxin production from untransfected (Cont), Ad-IL-13Rα2 (30 moi)-transfected, or Ad-LacZ (30-moi)-transfected BEAS-2B cells 24 h after stimulation with IL-13 (left), or the indicated time after IL-13 stimulation (50 ng/ml, right). Values are means ± SEM, $n = 5$. (D) After transfection with Ad-IL-13Rα2 or Ad-LacZ (30 moi), soluble IL-13Rα2 in the supernatant of BEAS-2B cells was quantified by ELISA. Values are means ± SEM, $n = 5$.

from the cell surface after full-length IL-13Rα2 transfection (Fig. 1D).

Functional analysis of soluble IL-13Rα2

We next examined the inhibitory effects of soluble IL-13Rα2 on IL-13-induced eotaxin expression. The transfer of the 3-day cell culture media (referred to as conditioned media) to other un-transfected BEAS-2B cells slightly but significantly attenuated IL-13-induced eotaxin production (Fig. 2A). The transfer of the cell culture media collected just after the transfection to other un-transfected BEAS-

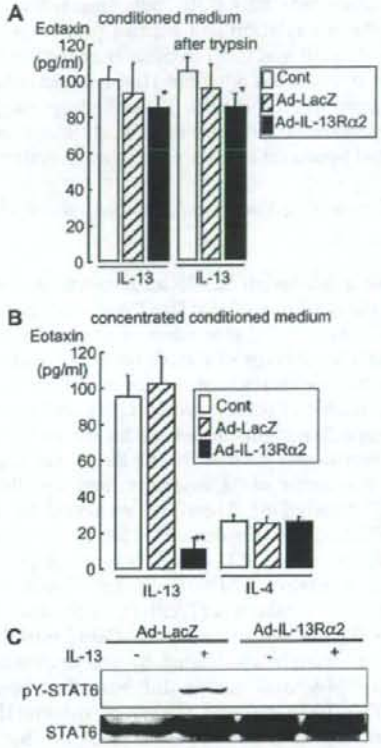

Fig. 2. Soluble IL-13Rα2 suppresses IL-13-induced eotaxin expression and STAT6 activation in human airway epithelial cells. (A) Three days after the transfection of Ad-IL-13Rα2 (30-moi) or Ad-LacZ (30-moi), the overlying cell culture medium (conditioned medium) was removed. The conditioned medium was transferred to untransfected BEAS-2B cells and stimulated with IL-13 (10 ng/ml) for 24 h. Eotaxin levels in the supernatant were measured. Values are means ± SEM, $n = 5$. $^{*}P < 0.05$; $^{**}P < 0.01$, compared with conditioned media from untransfected cells. (B) Three days after the transfection of Ad-IL-13Rα2 (30 moi) or Ad-LacZ (30 moi), the overlying cell culture medium (conditioned medium) was removed. The concentrated conditioned medium (one-seventh of the original volume) was transferred to untransfected BEAS-2B cells and stimulated with IL-13 (10 ng/ml) or IL-4 (10 ng/ml) for 24 h. Eotaxin levels in the supernatant were measured. Values are means ± SEM, $n = 5$. $^{*}P < 0.05$; $^{**}P < 0.01$, compared with concentrated conditioned media from untransfected cells. (C) The concentrated conditioned medium was transferred to untransfected BEAS-2B cells and stimulated with IL-13 (10 ng/ml) for 30 min. Cell extracts were immunoblotted with the indicated antibodies.

2B cells did not affect IL-13-induced eotaxin production. Furthermore, Ad-IL-13Rα2-transfected cells were re-seeded after trypsin treatment to remove Ad-IL-13Rα2 vectors, and the concentrated 3-day cell culture media of re-seeded cells also inhibited IL-13-induced eotaxin production in other cells (Fig. 2A). These results suggest that an inhibitory effect of cell culture media is not due to re-transfection of Ad-IL-13Rα2.

Conditioned media were then concentrated to about one-seventh of the original volume by centrifugal filtration. The transfer of the concentrated 3-day conditioned media to un-transfected BEAS-2B cells markedly inhibited STAT6 phosphorylation and eotaxin production induced by IL-13 (Fig. 2B and C). The transfer of the concentrated conditioned media did not affect IL-4-induced eotaxin production from BEAS-2B cells. These findings suggest that soluble mediator(s) released after IL-13Rα2 transfection inhibit IL-13-induced eotaxin expression in epithelial cells.

Effect of protease inhibitor and PMA on soluble IL-13Rα2 release

Because a full-length IL-13Rα2 gene was transfected to the cells, the detection of IL-13Rα2 in the cell culture medium may implicate the generation of soluble IL-13Rα2 by the proteolytic cleavage of surface receptors. In most cases of the proteolytic cleavage of surface receptors, PMA stimulates the release of soluble proteins [24], and many PMA-induced shedding events have been known to be mediated by metalloproteases such as the TNFα-converting enzyme (TACE), a member of "a disintegrin and metalloprotease (ADAM)" family [16]. Therefore, we tested the effect of PMA on the release of soluble IL-13Rα2 and whether the PMA-induced release of IL-13Rα2 is sensitive to the metalloprotease inhibitor GM6001, to the TACE inhibitor TNFα protease inhibitor-1 (TAPI-1), or to other protease inhibitors. The release of soluble IL-13Rα2 into the supernatant was strongly accelerated by the treatment of the cells with PMA, and vehicle did not affect soluble IL-13Rα2. This PMA-induced release of soluble IL-13Rα2 was markedly inhibited by GM6001 or by TAPI-1 (Fig. 3). Serine protease inhibitor (aprotinin), cysteine protease inhibitor (leupeptin), or amniopeptidase B inhibitor (bestatin) did not affect the PMA-induced release of IL-13Rα2 (Fig. 3). These findings imply that endogenous metalloprotease(s) activate the solubilization of IL-13Rα2.

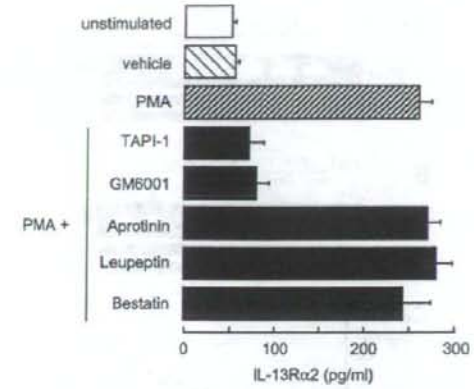

Fig. 3. Inhibition of soluble IL-13Rα2 generation from Ad-IL-13Rα2 transfected cells by protease inhibitors. Transfected BEAS-2B cells (Ad-IL-13Rα2, 30 moi) were pretreated with TAP-1 (30 μM), GM6001 (10 μM), aprotinin (1 μM), leupeptin (100 μM), or bestatin (10 μM) for 30 min and then stimulated with PMA (10 ng/ml) for 2 h. Supernatants were collected for the measurement of soluble IL-13Rα2 by ELISA. Values are means ± SEM, $n = 3$.

Discussion

We demonstrate that the transfection of full-length IL-13Rα2 induces the release of soluble IL-13Rα2 from airway epithelial cells and that the transfer of conditioned media from IL-13Rα2-transfected cells inhibits IL-13-induced eotaxin production and STAT6 phosphorylation in other non-transfected cells. PMA enhances the release of soluble IL-13Rα2, and metalloprotease inhibitors block this PMA-induced release of IL-13Rα2. These findings suggest that the upregulation of membrane-bound IL-13Rα2 in airway epithelial cells secretes soluble IL-13Rα2 into its supernatant, leading to downregulation of the IL-13/STAT6 signal, and that a group of endogenous metalloproteases is responsible for the generation of soluble IL-13Rα2.

Soluble IL-13Rα2 might be generated by some mechanisms, including the proteolytic cleavage of a membrane-bound receptor and the alternative splicing of mRNA transcripts in humans. Many PMA-induced releases of soluble receptors have been known to be mediated by metalloproteases [16]. In the present study, the PMA-induced release of endogenous IL-13Rα2 is blocked by metalloprotease inhibitors in airway epithelial cells. Matrix metalloproteinases, membrane-tethered matrix metalloproteinases, and zinc-dependent ADAM family metalloproteinases have been shown to be responsible for the cleavage of the majority of shed proteins [25]. Among these, members of the ADAM family are particularly important [25,26]. TACE (ADAM17) has surfaced recently as a central mammalian ectodomain sheddase [26], and TACE acts on ectodomain cleavage and shedding of cytokine receptors, such as TNF receptors, the IL-6R α-chain, and the IL-15 α-chain [16]. IL-13 is a potent inducer of a variety of MMP moieties, including MMP-2, -8, -9, -12, -13, and -14 [27,28]. MMP-12 has an inhibitory role on eosinophil and macrophage accumulation in the generation of IL-13-induced inflammation, while MMP-9 inhibits neutrophil accumulation [29]. MMP-9 and MMP-12 can be considered downstream mediators and regulators of the IL-13-induced inflammatory response. The expression and/or activation of metalloproteinases, including TACE, might be also regulated by IL-13. Deregulation of metalloproteinases and soluble IL-13Rα2 secretion may take part in the pathophysiology of asthma.

The soluble form of IL-13Rα2 is reported to be generated by alternative splicing in the murine system [30]. In this report, however, several mouse organs expressed two IL-13Rα2 transcripts: the longer full-length protein and the shorter transcript lacking the transmembrane region exon10. Conditioned medium from transfectants expressing only the full-length transcript did contain detectable soluble IL-13Rα2, although the levels were lower than those of the transfectants expressing the shorter transcript [30]. These results indicate that the generation of soluble IL-13Rα2 can occur from the cleavage of membrane IL-13Rα2 in addition to an alternative transcript encoding a soluble form.

It has been reported that the release of an exosome-like vesicle acts as an alternative mechanism for the generation of soluble TNF receptor 1 [31]. Conditioned medium of epithelial cells after the transfection of IL-13Rα2 might contain full-length IL-13Rα2 in exosome-like vesicles. In the present study, PMA stimulated the release of IL-13Rα2 and metalloprotease inhibitors inhibited this release, suggesting that an increase in IL-13Rα2 in conditioned media is due to the proteolytic cleavage of the membrane-bound receptor but not due to the release of exosome-like vesicles.

IL-13Rα2 exists intracellularly, on the cell-surface membrane, and in soluble form. Although it has been shown that surface IL-13Rα2 is spontaneously released into the medium [32], the inhibitory action of the soluble form after enhanced expression of the full-length IL-13Rα2 chain has not yet been certified. In the present study, we demonstrate that airway epithelial cells after the upregulation of surface IL-13Rα2 release soluble IL-13Rα2, indicating that soluble IL-13Rα2 is a transferable inhibitor of IL-13 response in the human system.

In summary, we found that the airway epithelial cells with upregulation of membrane-bound IL-13Rα2 secrete biologically active soluble IL-13Rα2, which can effectively inhibit IL-13/STAT6 signals. A group of endogenous metalloproteases is responsible for the generation of soluble IL-13Rα2. Allergic airway inflammation may modulate the expression of these proteases and their inhibitors in addition to IL-13Rα2 expression. Further studies are warranted to further elucidate the mechanisms that regulate the generation of soluble IL-13Rα2.

Acknowledgments

We thank Ayako Hashizume, Tomoko Yoshimura, Yuki Yoshiura, and the Morphology Core, Faculty of Medicine, Kyushu University, for technical assistance.

References

[1] G. Grunig, M. Warnock, A.E. Wakil, R. Venkayya, F. Brombacher, D.M. Rennick, D. Sheppard, M. Mohrs, D.D. Donaldson, R.M. Locksley, D.B. Corry, Requirement for IL-13 independently of IL-4 in experimental asthma, Science 282 (1998) 2261–2263.

[2] M. Wills-Karp, J. Luyimbazi, X. Xu, B. Schofield, T.Y. Neben, C.L. Karp, D.D. Donaldson, Interleukin-13: central mediator of allergic asthma, Science 282 (1998) 2258–2261.

[3] Z. Zhu, R.J. Homer, Z. Wang, Q. Chen, G.P. Geba, J. Wang, Y. Zhang, J.A. Elias, Pulmonary expression of interleukin-13 causes inflammation, mucus hypersecretion, subepithelial fibrosis, physiologic abnormalities, and eotaxin production, J. Clin. Invest. 103 (1999) 779–788.

[4] M.J. Aman, N. Tayebi, N.I. Obiri, R.K. Puri, W.S. Modi, W.J. Leonard, cDNA cloning and characterization of the human interleukin 13 receptor alpha chain, J. Biol. Chem. 271 (1996) 29265–29270.

[5] D.J. Hilton, J.G. Zhang, D. Metcalf, W.S. Alexander, N.A. Nicola, T.A. Willson, Cloning and characterization of a binding subunit of the interleukin 13 receptor that is also a component of the interleukin 4 receptor, Proc. Natl. Acad. Sci. USA 93 (1996) 497–501.

[6] B. Miloux, P. Laurent, O. Bonnin, J. Lupker, D. Caput, N. Vita, P. Ferrara, Cloning of the human IL-13R alpha1 chain and reconstitution with the IL4R alpha of a functional IL-4/IL-13 receptor complex, FEBS Lett. 401 (1997) 163–166.

[7] D. Caput, P. Laurent, M. Kaghad, J.M. Lelias, S. Lefort, N. Vita, P. Ferrara, Cloning and characterization of a specific interleukin (IL)-13 binding protein structurally related to the IL-5 receptor alpha chain, J. Biol. Chem. 271 (1996) 16921–16926.

[8] D.D. Donaldson, M.J. Whitters, L.J. Fitz, T.Y. Neben, H. Finnerty, S.L. Henderson, R.M. O'Hara Jr., D.R. Beier, K.J. Turner, C.R. Wood, M. Collins, The murine IL-13 receptor alpha 2: molecular cloning, characterization, and comparison with murine IL-13 receptor alpha 1, J. Immunol. 161 (1998) 2317–2324.

[9] K. Kawakami, J. Taguchi, T. Murata, R.K. Puri, The interleukin-13 receptor alpha2 chain: an essential component for binding and internalization but not for interleukin-13-induced signal transduction through the STAT6 pathway, Blood 97 (2001) 2673–2679.

[10] K. Kawakami, F. Takeshita, R.K. Puri, Identification of distinct roles for a dileucine and a tyrosine internalization motif in the interleukin (IL)-13 binding component IL-13 receptor alpha 2 chain, J. Biol. Chem. 276 (2001) 25114–25120.

[11] M.G. Chiaramonte, M. Mentink-Kane, B.A. Jacobson, A.W. Cheever, M.J. Whitters, M.E. Goad, A. Wong, M. Collins, D.D. Donaldson, M.J. Grusby, T.A. Wynn, Regulation and function of the interleukin 13 receptor alpha 2 during a T helper cell type 2-dominant immune response, J. Exp. Med. 197 (2003) 687–701.

[12] N. Wood, M.J. Whitters, B.A. Jacobson, J. Witek, J.P. Sypek, M. Kasaian, M.J. Eppihimer, M. Unger, T. Tanaka, S.J. Goldman, M. Collins, D.D. Donaldson, M.J. Grusby, Enhanced interleukin (IL)-13 responses in mice lacking IL-13 receptor alpha 2, J. Exp. Med. 197 (2003) 703–709.

[13] S. Fichtner-Feigl, W. Strober, K. Kawakami, R.K. Puri, A. Kitani, IL-13 signaling through the IL-13alpha(2) receptor is involved in induction of TGF-beta(1) production and fibrosis, Nat. Med. (2005).

[14] M.O. Daines, G.K. Hershey, A novel mechanism by which interferon-gamma can regulate interleukin (IL)-13 responses. Evidence for intracellular stores of IL-13 receptor alpha -2 and their rapid mobilization by interferon-gamma, J. Biol. Chem. 277 (2002) 10387–10393.

[15] M. Kioi, S. Seetharam, R.K. Puri, N-linked glycosylation of IL-13R alpha2 is essential for optimal IL-13 inhibitory activity, FASEB J. 20 (2006) 2378–2380.

[16] S.J. Levine, Mechanisms of soluble cytokine receptor generation, J. Immunol. 173 (2004) 5343–5348.

[17] Y. Nishizuka, Studies and perspectives of protein kinase C, Science 233 (1986) 305–312.

[18] M. Saito, T. Murata, K. Watanabe, K. Kawakami, M. Suzuki, T. Koji, R.K. Puri, K. Kitazato, N. Kobayashi, Adenoviral vector-mediated gene transfer of IL-13Ralpha2 chain followed by IL-13 cytotoxin treatment offers potent targeted therapy for cytotoxin-resistant cancers, Int. J. Cancer 116 (2005) 1–8.

[19] T. Nakano, H. Inoue, S. Fukuyama, K. Matsumoto, M. Matsumura, M. Tsuda, T. Matsumoto, H. Aizawa, Y. Nakanishi, Niflumic acid

suppresses interleukin-13-induced asthma phenotypes, Am. J. Respir. Crit. Care Med. 173 (2006) 1216–1221.
[20] H. Inoue, R. Kato, S. Fukuyama, A. Nonami, K. Taniguchi, K. Matsumoto, T. Nakano, M. Tsuda, M. Matsumura, M. Kubo, F. Ishikawa, B.G. Moon, K. Takatsu, Y. Nakanishi, A. Yoshimura, Spred-1 negatively regulates allergen-induced airway eosinophilia and hyperresponsiveness, J. Exp. Med. 201 (2005) 73–82.
[21] J. Hoeck, M. Woisetschlager, STAT6 mediates eotaxin-1 expression in IL-4 or TNF-alpha-induced fibroblasts, J. Immunol. 166 (2001) 4507–4515.
[22] S. Matsukura, C. Stellato, S.N. Georas, V. Casolaro, J.R. Plitt, K. Miura, S. Kurosawa, U. Schindler, R.P. Schleimer, Interleukin-13 upregulates eotaxin expression in airway epithelial cells by a stat6-dependent mechanism, Am. J. Respir. Cell Mol. Biol. 24 (2001) 755–761.
[23] J. Bernard, D. Treton, C. Vermot-Desroches, C. Boden, P. Horellou, E. Angevin, P. Galanaud, J. Wijdenes, Y. Richard, Expression of interleukin 13 receptor in glioma and renal cell carcinoma: IL-13Ralpha2 as a decoy receptor for IL-13, Lab Invest. 81 (2001) 1223–1231.
[24] J. Arribas, A. Borroto, Protein ectodomain shedding, Chem. Rev. 102 (2002) 4627–4638.
[25] N.M. Hooper, E.H. Karran, A.J. Turner, Membrane protein secretases, Biochem. J. 321 (Pt 2) (1997) 265–279.
[26] J.J. Peschon, J.L. Slack, P. Reddy, K.L. Stocking, S.W. Sunnarborg, D.C. Lee, W.E. Russell, B.J. Castner, R.S. Johnson, J.N. Fitzner, R.W. Boyce, N. Nelson, C.J. Kozlosky, M.F. Wolfson, C.T. Rauch, D.P. Cerretti, R.J. Paxton, C.J. March, R.A. Black, An essential role for ectodomain shedding in mammalian development, Science 282 (1998) 1281–1284.
[27] N.E. King, N. Zimmermann, S.M. Pope, P.C. Fulkerson, N.M. Nikolaidis, A. Mishra, D.P. Witte, M.E. Rothenberg, Expression and regulation of a disintegrin and metalloproteinase (ADAM) 8 in experimental asthma, Am. J. Respir. Cell Mol. Biol. 31 (2004) 257–265.
[28] T. Zheng, Z. Zhu, Z. Wang, R.J. Homer, B. Ma, R.J. Riese Jr., H.A. Chapman Jr., S.D. Shapiro, J.A. Elias, Inducible targeting of IL-13 to the adult lung causes matrix metalloproteinase- and cathepsin-dependent emphysema, J. Clin. Invest. 106 (2000) 1081–1093.
[29] S. Lanone, T. Zheng, Z. Zhu, W. Liu, C.G. Lee, B. Ma, Q. Chen, R.J. Homer, J. Wang, L.A. Rabach, M.E. Rabach, J.M. Shipley, S.D. Shapiro, R.M. Senior, J.A. Elias, Overlapping and enzyme-specific contributions of matrix metalloproteinases-9 and -12 in IL-13-induced inflammation and remodeling, J. Clin. Invest. 110 (2002) 463–474.
[30] Y. Tabata, W. Chen, M.R. Warrier, A.M. Gibson, M.O. Daines, G.K. Hershey, Allergy-driven alternative splicing of IL-13 receptor alpha2 yields distinct membrane and soluble forms, J. Immunol. 177 (2006) 7905–7912.
[31] F.I. Hawari, F.N. Rouhani, X. Cui, Z.X. Yu, C. Buckley, M. Kaler, S.J. Levine, Release of full-length 55-kDa TNF receptor 1 in exosome-like vesicles: a mechanism for generation of soluble cytokine receptors, Proc. Natl. Acad. Sci. USA 101 (2004) 1297–1302.
[32] M.O. Daines, Y. Tabata, B.A. Walker, W. Chen, M.R. Warrier, S. Basu, G.K. Hershey, Level of expression of IL-13R alpha 2 impacts receptor distribution and IL-13 signaling, J. Immunol. 176 (2006) 7495–7501.

ATF4-Mediated Induction of 4E-BP1 Contributes to Pancreatic β Cell Survival under Endoplasmic Reticulum Stress

Suguru Yamaguchi,[1,3] Hisamitsu Ishihara,[1,*] Takahiro Yamada,[1] Akira Tamura,[1] Masahiro Usui,[1] Ryu Tominaga,[1] Yuichiro Munakata,[1] Chihiro Satake,[1] Hideki Katagiri,[2] Fumi Tashiro,[4] Hiroyuki Aburatani,[5] Kyoko Tsukiyama-Kohara,[6] Jun-ichi Miyazaki,[4] Nahum Sonenberg,[7] and Yoshitomo Oka[1]

[1]Division of Molecular Metabolism and Diabetes
[2]Division of Advanced Therapeutics for Metabolic Diseases, Center for Translational and Advanced Animal Research
Tohoku University Graduate School of Medicine, Sendai, Miyagi 980-8575, Japan
[3]Institute for International Advanced Research and Education, Tohoku University, Sendai, Miyagi 980-8578, Japan
[4]Division of Stem Cell Regulation Research, Osaka University Graduate School of Medicine, Suita, Osaka 565-0871, Japan
[5]Research Center for Advanced Science and Technology, University of Tokyo, Tokyo 153-8904, Japan
[6]Department of Experimental Phylaxiology, Faculty of Medical and Pharmaceutical Sciences, Kumamoto University, Kumamoto 860-8556, Japan
[7]Department of Biochemistry and McGill Cancer Centre, McGill University, Montreal, QC H3G 1Y6, Canada
*Correspondence: hisamitsu-ishihara@mail.tains.tohoku.ac.jp
DOI 10.1016/j.cmet.2008.01.008

SUMMARY

Endoplasmic reticulum (ER) stress-mediated apoptosis may play a crucial role in loss of pancreatic β cell mass, contributing to the development of diabetes. Here we show that induction of 4E-BP1, the suppressor of the mRNA 5′ cap-binding protein eukaryotic initiation factor 4E (eIF4E), is involved in β cell survival under ER stress. 4E-BP1 expression was increased in islets under ER stress in several mouse models of diabetes. The *Eif4ebp1* gene encoding 4E-BP1 was revealed to be a direct target of the transcription factor ATF4. Deletion of the *Eif4ebp1* gene increased susceptibility to ER stress-mediated apoptosis in MIN6 β cells and mouse islets, which was accompanied by deregulated translational control. Furthermore, *Eif4ebp1* deletion accelerated β cell loss and exacerbated hyperglycemia in mouse models of diabetes. Thus, 4E-BP1 induction contributes to the maintenance of β cell homeostasis during ER stress and is a potential therapeutic target for diabetes.

INTRODUCTION

Recent studies have shown decreased pancreatic β cell mass to be a common feature of subjects with type 2 diabetes mellitus (Butler et al., 2003). Susceptibility to stress-induced apoptosis may underlie β cell loss. Translational regulation is an essential strategy by which cells cope with stress conditions (Clemens, 2001). Translation of eukaryotic mRNA is regulated primarily at the level of initiation. Translational initiation begins with formation of a ternary complex composed of the methionine-charged initiator tRNA, eukaryotic initiation factor 2 (eIF2), and GTP (Holcik and Sonenberg, 2005). The ternary complex then binds to the 40S ribosomal subunit and several other initiation factors, generating the 43S preinitiation complex. The mRNA 5′ cap-binding protein eIF4E associates with eIF4A and eIF4G to form the eIF4F complex and interacts with the 5′ cap structure of the mRNA. The eIF4F complex then recruits the 43S preinitiation complex to the mRNA, allowing the complex to scan toward the initiator AUG codon. The two best characterized regulatory steps in this translational control are formation of the ternary complex and assembly of the eIF4F complex. Phosphorylation of the α subunit of eIF2 (eIF2α) prevents ternary complex formation and thereby suppresses global translation. In addition, eIF4E-binding proteins (4E-BPs) inhibit eIF4F assembly by competitively displacing eIF4G from eIF4E. Global translational suppression through eIF2α phosphorylation is a mechanism shared among different stress-response pathways. Depending on the nature of the stress stimulus, eIF2α can be phosphorylated by four different kinases (Holcik and Sonenberg, 2005). Global attenuation of protein biosynthesis then paradoxically increases expression of several proteins, including the transcription factor ATF4 (Harding et al., 2000).

Because of their high insulin secretory activity, β cells are vulnerable to endoplasmic reticulum (ER) stress, a condition of disrupted ER homeostasis due to accumulation of misfolded proteins (Schroder and Kaufman, 2005). Cells respond to ER stress by activating an adaptive cellular response known as the unfolded protein response (UPR). Under ER stress conditions, global translation is suppressed through eIF2α phosphorylation by an ER-resident kinase, PERK. The importance of PERK-mediated translational suppression has been demonstrated in infancy-onset diabetes and skeletal defects caused by loss of PERK in humans (Delepine et al., 2000) and mice (Harding et al., 2001; Zhang et al., 2002). However, the roles of translational control through inhibition of eIF4F assembly by 4E-BPs under stress conditions, including ER stress, have yet to be fully clarified. Herein, we have studied roles of 4E-BP1,

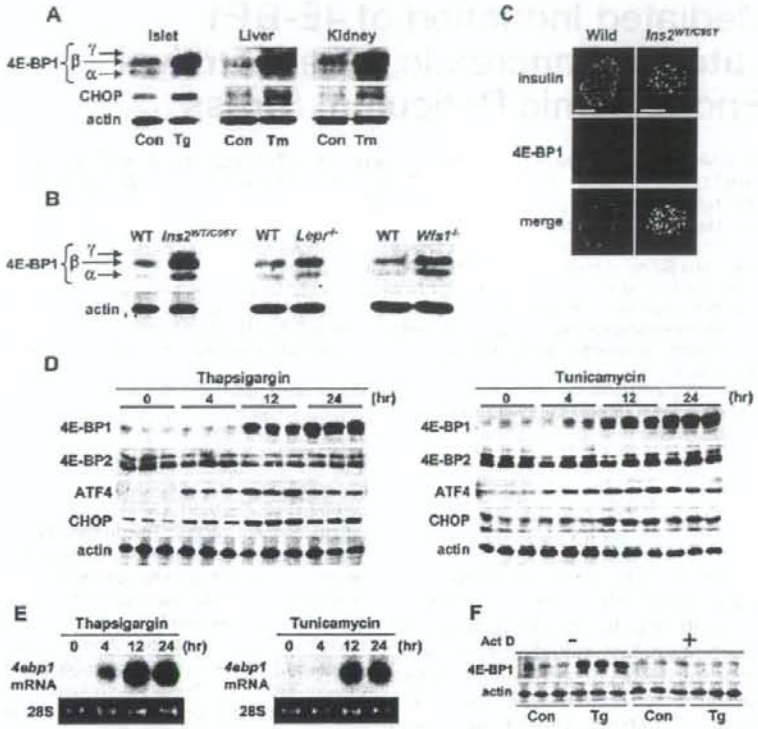

Figure 1. ER Stress Induces 4E-BP1 Expression

(A) Expression of 4E-BP1 protein in isolated islets treated with vehicle (0.05% DMSO) control (Con) or 0.5 μM thapsigargin (Tg) for 12 hr. 4E-BP1 expression was also examined in the livers and kidneys of mice that had received intraperitoneal injections of tunicamycin (Tm) 96 hr previously.

(B) Expression of 4E-BP1 protein in islets from wild-type (WT), *Ins2*$^{WT/C96Y}$, *Lepr*$^{-/-}$, and *Wfs1*$^{-/-}$ mice.

(C) Immunostaining of pancreatic sections from WT and *Ins2*$^{WT/C96Y}$ mice using anti-insulin and anti-4E-BP1 antibodies. Scale bars = 50 μm.

(D and E) Time courses of 4E-BP1, 4E-BP2, ATF4, and CHOP expression (D) and *4ebp1* mRNA expression (E) in MIN6 cells treated with thapsigargin (left panel) or tunicamycin (right).

(F) Inhibition of 4E-BP1 induction by actinomycin D (1 μg/ml) in MIN6 cells treated with thapsigargin for 12 hr.

one of three isoforms of the 4E-BP family, in β cells under ER stress.

RESULTS

ER Stress Induces 4E-BP1

4E-BP1 protein is present in three forms with different phosphorylation states. The hypophosphorylated α and β forms are active and the hyperphosphorylated γ form is inactive in terms of eIF4E binding. Expression of 4E-BP1 protein, especially the hypophosphorylated forms, was markedly induced, with an increase in CHOP, a stress marker protein, in isolated islets treated with thapsigargin (an ER Ca^{2+} pump inhibitor causing ER stress) (Figure 1A). 4E-BP1 induction was also observed in liver and kidneys of mice administered tunicamycin (a protein glycosylation inhibitor), another ER stress inducer (Figure 1A).

Furthermore, 4E-BP1 protein expression was markedly increased in *Ins2*$^{WT/C96Y}$ islets (Figures 1B and 1C), in which misfolded insulin molecules with a C96Y mutation cause ER stress (Wang et al., 1999). Islets from leptin receptor null (*Lepr*$^{-/-}$) mice, which have been shown to suffer from ER stress (Laybutt et al., 2007), also exhibited increased 4E-BP1 expression (Figure 1B). The *Wfs1*$^{-/-}$ mouse (Ishihara et al., 2004) is a model of Wolfram syndrome, which is characterized by juvenile-onset diabetes mellitus and optic atrophy and is caused by *WFS1* mutations (Inoue et al., 1998; Strom et al., 1998). WFS1-deficient islets are affected by chronic ER stress (Ishihara et al., 2004; Riggs et al., 2005). Again, 4E-BP1 protein was increased in *Wfs1*$^{-/-}$ islets (Figure 1B).

Induction of 4E-BP1 by ER stress was also observed in insulinoma MIN6 cells (Miyazaki et al., 1990) (Figure 1D). Expression of 4E-BP2, another member of the 4E-BP family, remained unchanged. While expression of ATF4 and CHOP peaked at 12 hr after treatment with thapsigargin or tunicamycin, 4E-BP1 protein was further increased at 24 hr posttreatment (Figure 1D). 4E-BP1 protein induction appeared to result from transcriptional

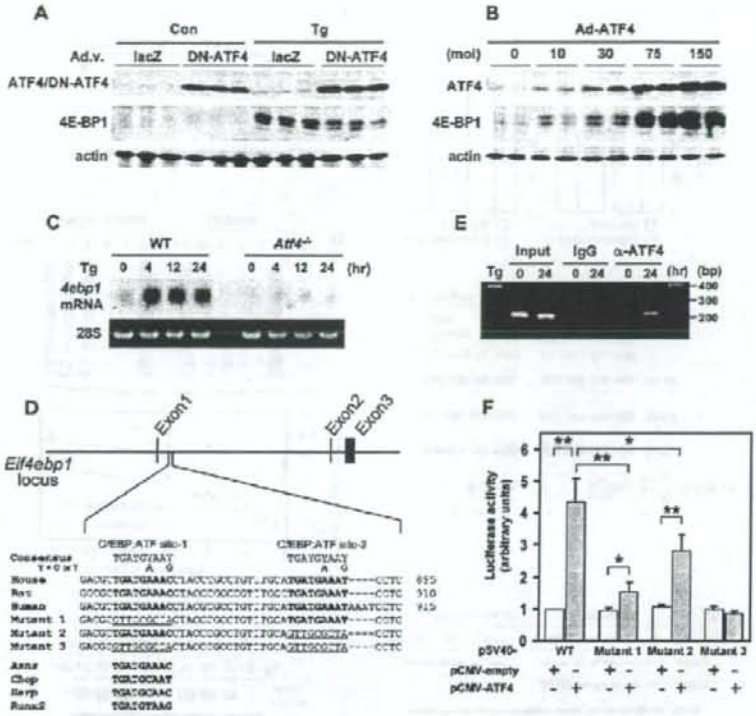

Figure 2. *Eif4ebp1* Is a Direct Target of ATF4

(A) Suppression of thapsigargin (Tg, 0.5 μM)-induced 4E-BP1 expression by dominant-negative ATF4 (DN-ATF4). MIN6 cells were infected with an adenovirus expressing either lacZ or DN-ATF4. Two days later, the cells were treated with vehicle (0.05% DMSO) control (Con) or Tg for 12 hr.

(B) 4E-BP1 expression in MIN6 cells infected with an adenovirus expressing wild-type ATF4 at the indicated multiplicity of infection (moi).

(C) *4ebp1* mRNA levels in wild-type and *Atf4*$^{-/-}$ MEFs treated with thapsigargin.

(D) C/EBP:ATF composite sites in intron 1 of the *Eif4ebp1* gene. Mouse, rat, and human *Eif4ebp1* gene segments are aligned with ATF4 binding sequences in several genes. Numbers are positions relative to A of the initial ATG codon. *Asns*, asparagine synthetase; *Herp*, homocysteine-induced ER protein; *Runx2*, runt-related transcription factor 2.

(E) Chromatin immunoprecipitation assay of MIN6 cells treated with thapsigargin. DNAs precipitated with nonspecific or anti-ATF4 IgG were amplified using primers for the *Eif4ebp1* intron 1 region.

(F) ATF4 induction of luciferase reporters with the *SV40* promoter and an *Eif4ebp1* gene segment with C/EBP:ATF composite sites or their mutants shown in (D). MIN6 cells were transfected with luciferase reporters together with either pCMV-empty or pCMV-ATF4. Error bars represent SEM. n = 4; *p < 0.05, **p < 0.01.

activation since *4ebp1* mRNA levels were also increased by these ER stress inducers (Figure 1E) and the transcriptional inhibitor actinomycin D completely blocked 4E-BP1 induction by thapsigargin (Figure 1F).

ATF4 Directly Activates the *Eif4ebp1* Gene

MIN6 cells were infected with recombinant adenoviruses expressing dominant-negative (DN) forms of transcription factors involved in the UPR. Expression of DN-ATF4 (He et al., 2001) (Figure 2A), but not DN-ATF6 or DN-XBP1 (see Figure S1 available online), suppressed 4E-BP1 induction by thapsigargin. Conversely, expression of wild-type ATF4 dramatically induced 4E-BP1 expression (Figure 2B). Furthermore, *4ebp1* mRNA levels were not increased by thapsigargin in *Atf4*$^{-/-}$ murine embryonic fibroblasts (MEFs) (Harding et al., 2003) (Figure 2C).

A survey of the mouse *Eif4ebp1* gene using a luciferase assay identified a segment in intron 1 that conferred thapsigargin sensitivity to a luciferase reporter (Figure S2). Indeed, we found two potential ATF4 binding sequences (C/EBP:ATF composite sites) in this segment (Figure 2D). Chromatin immunoprecipitation (ChIP) assays revealed that ATF4 binds this segment (Figure 2E). Furthermore, cotransfection of a luciferase reporter containing the C/EBP:ATF sites with an ATF4-expressing plasmid increased luciferase activity by 4.3-fold (Figure 2F). Disruption of the upstream C/EBP:ATF site (mutant 1) or the downstream site (mutant 2) decreased the ATF4-mediated increase in luciferase activity by 83% or 47%, respectively, and disruption of both (mutant 3) completely abolished the increase (Figure 2F).

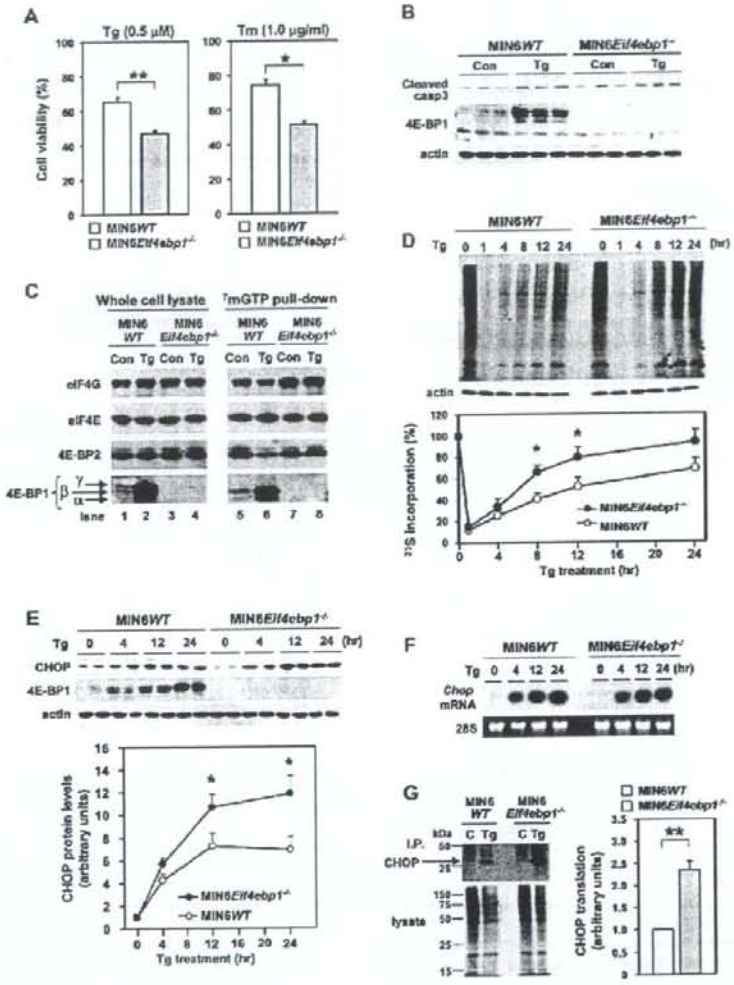

Figure 3. 4E-BP1-Deficient Cells Exhibit Increased Apoptosis Susceptibility with Deregulated Translational Control

(A) Viability of MIN6*WT* and MIN6*Eif4ebp1*$^{-/-}$ cells treated with 0.5 μM thapsigargin (Tg) or 1.0 μg/ml tunicamycin (Tm) for 36 hr, normalized to MIN6*WT* cells treated with vehicle (0.05% DMSO). n = 3–4.

(B) Immunoblot of cleaved caspase-3 in MIN6*WT* and MIN6*Eif4ebp1*$^{-/-}$ cells treated with vehicle control (Con) or thapsigargin for 24 hr.

(C) Immunoblot analysis of 4E-BP1, 4E-BP2, eIF4E, and eIF4G in whole-cell lysates (left) or in a complex associated with ^{7}mGTP-Sepharose (right) in cells treated with thapsigargin for 24 hr.

(D) [^{35}S]methionine/cysteine incorporation during a 15 min pulse labeling in MIN6*WT* and MIN6*Eif4ebp1*$^{-/-}$ cells pretreated with thapsigargin for the indicated periods. Ten percent of the lysates were also probed with an anti-actin antibody. A representative autoradiogram is shown in the upper panel; data from three experiments are summarized in the lower panel.

(E) Increased CHOP induction in MIN6*Eif4ebp1*$^{-/-}$ cells treated with thapsigargin. Representative blots are shown in the upper panel; data from four experiments are summarized in the lower panel.

(F) *Chop* mRNA levels in MIN6*WT* and MIN6*Eif4ebp1*$^{-/-}$ cells treated with thapsigargin.

(G) Greater *Chop* translation in MIN6*Eif4ebp1*$^{-/-}$ cells treated with thapsigargin. MIN6*WT* and MIN6*Eif4ebp1*$^{-/-}$ cells treated with vehicle (C) or thapsigargin (Tg) for 12 hr were labeled with [^{35}S]methionine/cysteine. Lysates were either directly subjected to SDS-PAGE or immunoprecipitated with anti-CHOP antibody. Representative autoradiograms are shown in the left panel; data from four experiments are summarized in the right panel.

Error bars represent SEM. *$p < 0.05$, **$p < 0.01$.

4E-BP1-Deficient β Cells Are More Vulnerable to ER Stress

A 4E-BP1-deficient β cell line, MIN6*Eif4ebp1*$^{-/-}$, was established by crossing *Eif4ebp1*$^{-/-}$ mice (Tsukiyama-Kohara et al., 2001) with IT6 mice expressing SV40 large T antigen in β cells (Miyazaki et al., 1990). MIN6 cells with wild-type *Eif4ebp1* alleles, established in parallel, were designated MIN6*WT* cells. MIN6*Eif4ebp1*$^{-/-}$ cells were more vulnerable to ER stress inducers than MIN6*WT* cells (Figure 3A). 4E-BP1 re-expression restored this diminished viability of MIN6*Eif4ebp1*$^{-/-}$ cells to control levels (Figure S3A). The increased susceptibility to ER stress-induced cell death was accompanied by enhanced caspase-3 cleavage (Figure 3B), indicating that the reduced viability of MIN6*Eif4ebp1*$^{-/-}$ cells was due at least in part to increased apoptosis. In addition, DNA fragmentation under ER stress was greater in *Eif4ebp1*$^{-/-}$ islets than in wild-type islets (Figure S3B). These results suggest that 4E-BP1 induction contributes to β cell survival under ER stress.

We then examined the impact of 4E-BP1 deficiency on the integrity of the eIF4F translational initiation complex. Pull-down assays of eIF4E and its binding partners with a cap analog, 7-methyl-GTP, revealed that thapsigargin-induced 4E-BP1 expression resulted in marked increases in the amounts of hypophosphorylated 4E-BP1 α and β forms bound to eIF4E, displacing eIF4G from eIF4E in MIN6*WT* cells (Figure 3C, compare lane 5 with lane 6). The amount of eIF4G bound to eIF4E was reduced to 63% ± 3% ($n = 4$, $p < 0.05$) of that in vehicle-treated MIN6WT cells. In contrast, levels of eIF4G bound to eIF4E were not decreased by thapsigargin in MIN6*Eif4ebp1*$^{-/-}$ cells (Figure 3C, compare lane 7 with lane 8). Thus, eIF4E availability for translational initiation was greater in MIN6*Eif4ebp1*$^{-/-}$ cells than in MIN6*WT* cells under ER stress. Measurement of the global translation rate revealed that recovery from translational suppression by thapsigargin was more rapid in 4E-BP1-deficient cells (Figure 3D).

Translation of newly synthesized mRNA molecules is reportedly much more dependent on eIF4E availability than that of preexisting mRNAs (Novoa and Carrasco, 1999). Expression of CHOP, a mediator of ER stress-induced apoptosis, was thus studied in MIN6*Eif4ebp1*$^{-/-}$ cells since *Chop* mRNA is one of the transcripts most abundantly synthesized during ER stress (Pirot et al., 2007). *Eif4ebp1* deletion caused greater CHOP protein induction by thapsigargin in MIN6 cells (Figure 3E), with unaltered *Chop* mRNA accumulation (Figure 3F). Pulse-labeling experiments demonstrated enhanced CHOP translation (Figure 3G). Thus, CHOP expression during ER stress was augmented via increased translation in 4E-BP1 deficiency.

Eif4ebp1 Deletion Accelerates β Cell Loss in Mouse Diabetes Models

To examine the roles of 4E-BP1 under ER stress in vivo, *Eif4ebp1*$^{-/-}$ mice on the 129S6 background were fed a high-fat diet (HFD), which is thought to produce ER stress in β cells through peripheral insulin resistance (Scheuner et al., 2005). *Eif4ebp1*$^{-/-}$ mice developed glucose intolerance (Figures S4A and S4B), which was associated with blunted insulin secretion (Figure S4C) and reduced pancreatic insulin content (Figure S4D) as compared to HFD-fed wild-type mice. These data suggest that *Eif4ebp1*$^{-/-}$ mice have a β cell defect. However, HFD-fed *Eif4ebp1*$^{-/-}$ mice gained more weight and were more insulin resistant than HFD-fed wild-type mice (Figures S4E and S4F). Therefore, the possibility remains that β cell failure in HFD-fed *Eif4ebp1*$^{-/-}$ mice resulted from greater ER stress rather than from a defect in β cells lacking 4E-BP1.

We next crossed *Eif4ebp1*$^{-/-}$ mice with two genetic models of diabetes in which β cells are under ER stress, *Ins2*$^{WT/C96Y}$ and *Wfs1*$^{-/-}$ mice on the 129S6 background. 4E-BP1 deficiency did not alter body weight (Figures S5A and S5B) or insulin sensitivity (Figures S5C and S5D) but worsened hyperglycemia in *Ins2*$^{WT/C96Y}$ (Figure 4A) and *Wfs1*$^{-/-}$ (Figure 4B) mice. In *Eif4ebp1*$^{-/-}$ *Ins2*$^{WT/C96Y}$ mice, pancreatic insulin content was less than half of that in *Ins2*$^{WT/C96Y}$ mice at 5 weeks of age (Figure 4C), and the majority of islets in *Eif4ebp1*$^{-/-}$ *Ins2*$^{WT/C96Y}$ mice were smaller as compared to those in *Ins2*$^{WT/C96Y}$ mice (Figure 4D). We also observed a 38% decrease in pancreatic insulin content in *Eif4ebp1*$^{-/-}$ *Wfs1*$^{-/-}$ mice as compared to *Wfs1*$^{-/-}$ mice (Figure 4E). Importantly, the insulin-positive area was smaller in pancreatic sections from *Eif4ebp1*$^{-/-}$ *Wfs1*$^{-/-}$ mice than in pancreatic sections from *Wfs1*$^{-/-}$ mice at 27–30 weeks of age (Figure 4F), indicating that ER stress-mediated β cell loss is exacerbated by 4E-BP1 deficiency in vivo.

Global protein synthesis was studied in these mouse islets. A tendency toward decreased protein synthesis was observed in both *Ins2*$^{WT/C96Y}$ (Figure 4G, hatched bar; $p = 0.074$) and *Wfs1*$^{-/-}$ islets (Figure 4H, hatched bar; $p = 0.079$) as compared to wild-type islets. *Eif4ebp1* deletion ablated this regulation and resulted in significantly increased protein synthesis in *Eif4ebp1*$^{-/-}$ *Ins2*$^{WT/C96Y}$ ($p = 0.013$) and *Eif4ebp1*$^{-/-}$ *Wfs1*$^{-/-}$ ($p = 0.045$) islets as compared to that in corresponding single mutants (compared hatched with filled bars in Figures 4G and 4H). These data suggest that accelerated β cell loss under ER stress is due to deregulated translational control.

DISCUSSION

Our results implicate 4E-BP1, identified as a component of the UPR, in β cell survival under ER stress. Important roles of 4E-BPs under various stress conditions have been recently demonstrated in yeast (Ibrahimo et al., 2006) and *Drosophila* (Teleman et al., 2005; Tettweiler et al., 2005). These data suggest that translational suppression by 4E-BPs is an evolutionarily conserved strategy against stress conditions. Although we focused on β cells, ER stress-mediated induction of 4E-BP1 was also observed in the liver and kidneys, suggesting the general importance of the present findings.

Our results suggest that, in addition to translational regulation by eIF2α phosphorylation due to PERK activation, another mode of translational control mediated by 4E-BP1 plays a role in the maintenance of β cell homeostasis under ER stress. Since translational suppression by eIF2α phosphorylation is transient owing to feedback dephosphorylation by GADD34 (Novoa et al., 2001), prolonged translational suppression by 4E-BP1 might be needed in the later stages of the UPR. However, in contrast to PERK, 4E-BP1 deficiency alone does not cause diabetes in mice under normal conditions, suggesting that 4E-BP1 protein is not a key regulator but rather functions with other molecules to maintain β cell homeostasis under ER stress. The preferential role of 4E-BP1 in the later stages of the UPR might be puzzling since expression of

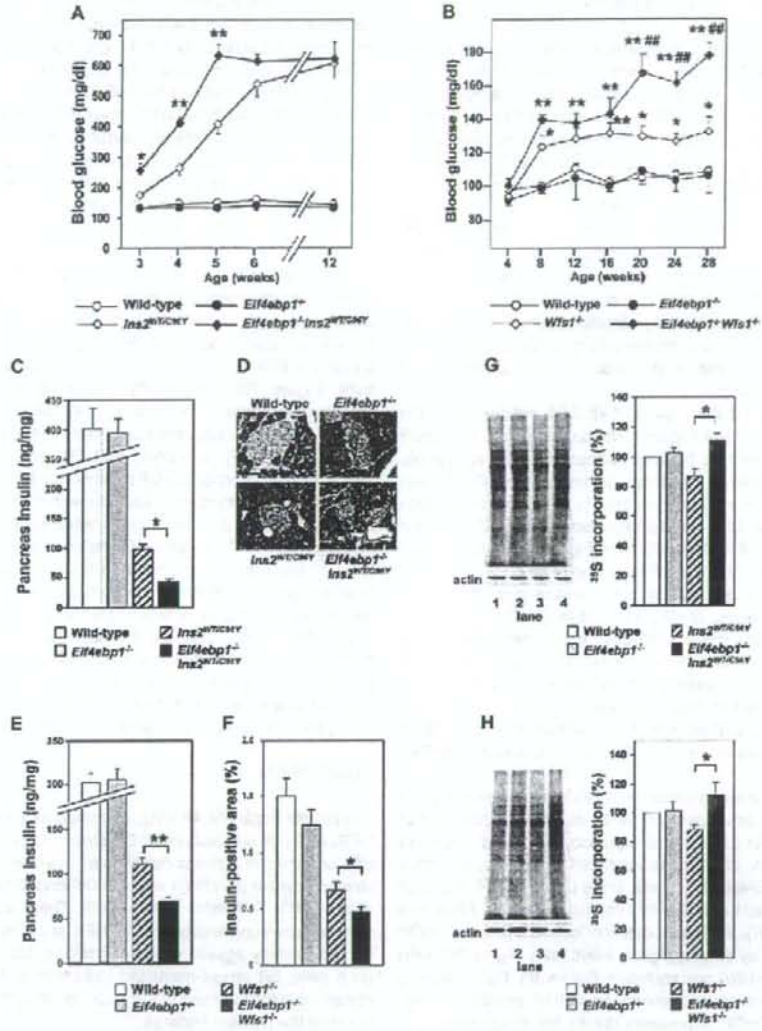

Figure 4. β Cell Loss Is Exacerbated by 4E-BP1 Deficiency in Mouse Diabetes Models

(A) Fed blood glucose levels of wild-type (n = 6), *Eif4ebp1*$^{-/-}$ (n = 5), *Ins2*$^{WT/C96Y}$ (n = 9), and *Eif4ebp1*$^{-/-}$ *Ins2*$^{WT/C96Y}$ (n = 11) mice. Data from three cohorts are combined. *p < 0.05, **p < 0.01 versus *Ins2*$^{WT/C96Y}$ mice.

(B) Fed blood glucose levels of wild-type (n = 12), *Eif4ebp1*$^{-/-}$ (n = 8), *Wfs1*$^{-/-}$ (n = 15), and *Eif4ebp1*$^{-/-}$ *Wfs1*$^{-/-}$ (n = 10) mice. Data from three cohorts are combined. *p < 0.05, **p < 0.01 versus wild-type mice; ##p < 0.01 versus *Wfs1*$^{-/-}$ mice.

(C) Pancreatic insulin content of mice of the indicated genotypes at 5 weeks of age. n = 3 for each genotype. *p < 0.05.

(D) Hematoxylin and eosin staining of sections showing representative islets from mice of the indicated genotypes at 5 weeks of age. Scale bars = 50 μm.

(E) Pancreatic insulin content of wild-type (n = 8), *Eif4ebp1*$^{-/-}$ (n = 4), *Wfs1*$^{-/-}$ (n = 15), and *Eif4ebp1*$^{-/-}$ *Wfs1*$^{-/-}$ (n = 12) mice at 27–30 weeks of age. **p < 0.01.

(F) Insulin-positive area in pancreatic sections of wild-type (n = 3), *Eif4ebp1*$^{-/-}$ (n = 3), *Wfs1*$^{-/-}$ (n = 4), and *Eif4ebp1*$^{-/-}$ *Wfs1*$^{-/-}$ (n = 5) mice at 27–30 weeks of age. *p < 0.05.

(G) [^{35}S]methionine/cysteine incorporation in islets of the indicated genotypes at 5–6 weeks of age. Ten percent of the lysates were also probed with an anti-actin antibody. A representative autoradiogram is shown in the left panel. Lane 1, wild-type; lane 2, *Eif4ebp1*$^{-/-}$; lane 3, *Ins2*$^{WT/C96Y}$; lane 4, *Eif4ebp1*$^{-/-}$ *Ins2*$^{WT/C96Y}$. Data from four experiments are summarized in the right panel. *p < 0.05.

ATF4, the primary inducer of *Eif4ebp1* under ER stress, is activated by translational suppression by eIF2α phosphorylation during the acute phase. We found that 4E-BP1 protein is stable with a half-life of approximately 20 hr (Figure S6). Thus, 4E-BP1 protein seems to continue to be expressed abundantly during the later stages of the UPR. This is consistent with the recent observation that several prosurvival proteins involved in the UPR are stable, while proapoptotic proteins are not (Rutkowski et al., 2006). We found that global protein synthesis was higher in 4E-BP1-deficient β cells than in wild-type cells under ER stress conditions. In particular, expression of CHOP was augmented in 4E-BP1 deficiency. Enhanced CHOP expression in 4E-BP1-deficient cells suggests that a reduction in eIF4E availability due to 4E-BP1 induction suppresses CHOP translation during ER stress in wild-type cells, possibly accounting for one of the mechanisms by which 4E-BP1 plays a role in adaptation to ER stress. Important roles of translational control via eIF4E availability have also been suggested in prolonged hypoxia (Koritzinsky et al., 2006). However, the signaling mechanisms for translational control are different: ER stress increases 4E-BP1 protein levels via ATF4 in β cells, while hypoxia enhances 4E-BP1 activity via dephosphorylation and also causes eIF4E nuclear localization in HeLa cells.

The present results also suggest that variations in genes regulating eIF4E availability and/or eIF4F formation may have an impact on susceptibility to diabetes. In this context, a recent report demonstrating that a gene encoding eIF4A2, a component of eIF4F, is possibly linked to type 2 diabetes in French families (Cheyssac et al., 2006) is of great interest. Furthermore, our findings raise the possibility that 4E-BP1 may be a potential target for diabetes mellitus treatment.

EXPERIMENTAL PROCEDURES

Animal Experiments

All animal experiments were approved by the Tohoku University Institutional Animal Care and Use Committee. *Wfs1*$^{-/-}$ mice were backcrossed to a 129S6 (Taconic) background for six generations. *Ins2*$^{WT/C96Y}$ mice (Charles River Laboratories) were backcrossed to a 129S6 background for five generations. *Eif4ebp1*$^{-/-}$ mice were maintained on a 129S6 background. Only male mice were used. For the in vivo studies shown in Figures 4A, 4C, and 4D, littermates from crosses of male *Ins2*$^{WT/C96Y}$ *Eif4ebp1*$^{+/-}$ and female *Ins2*$^{WT/WT}$ *Eif4ebp1*$^{+/-}$ mice were used. For Figures 4B, 4E, and 4F, littermates from intercrosses of *Eif4ebp1*$^{+/-}$ *Wfs1*$^{+/+}$ mice and littermates from intercrosses of *Eif4ebp1*$^{+/-}$ *Wfs1*$^{-/-}$ mice were used. For isolated islet experiments (Figures 4G and 4H), age-matched nonlittermate mice were used. To induce ER stress in vivo, mice were given a 0.5 μg/g body weight intraperitoneal injection of tunicamycin. After 96 hr, kidneys and livers were removed. Tissue sample processing, immunostaining of pancreatic sections, and determination of β cell area and pancreatic insulin content were performed as described previously (Ishihara et al., 2004).

Cell Culture and Cell Viability Assay

Pancreatic tumors in *Eif4ebp1*$^{-/-}$:SV40Tag mice on a mixed background were excised, yielding MIN6*Eif4ebp1*$^{-/-}$cells, which were used at 5–10 passages in this study. MIN6 cells were cultured in DMEM supplemented with 15% FCS. *Atf4*$^{-/-}$ MEFs were cultured in DMEM supplemented with a nonessential amino acid mixture and 10% FCS. Cells seeded in 24-well plates 2 days previously were treated with thapsigargin or tunicamycin and used for western blotting or cell viability assay. Cell viability was determined with a cell proliferation assay kit (Promega). Construction of adenoviruses and infection of MIN6 cells were performed as described previously (Ishihara et al., 2004).

Northern and Western Blotting and Cap-Binding Affinity Assay

Total RNA extracted using ISOGEN (Nippon Gene) was probed with ^{32}P-labeled cDNAs. Tissue homogenates and cell lysates were subjected to SDS-PAGE and probed with primary antibodies against 4E-BP1, 4E-BP2, eIF4E, eIF4G, cleaved caspase-3 (Cell Signaling), ATF4, CHOP (Santa Cruz), and actin (Sigma). Cell lysates were incubated with 7-methyl-GTP (^{7}mGTP)-Sepharose (Amersham) overnight at 4°C. The ^{7}mGTP-Sepharose was then pelleted and boiled. Experiments were performed at least three times. Band intensity was quantified using Scion Image software.

Metabolic Labeling

Due to the low islet yields from *Ins2*$^{WT/C96Y}$, *Ins2*$^{WT/C96Y}$ *Eif4ebp1*$^{-/-}$, *Wfs1*$^{-/-}$, and *Eif4ebp1*$^{-/-}$ *Wfs1*$^{-/-}$ mice, islets with these genotypes were pooled from two or three mice. Fifty to eighty islets were cultured for 3 days in RPMI supplemented with 10% FCS. Islets washed with methionine/cysteine-free RPMI containing 10% dialyzed FCS were labeled with a protein labeling mix (PerkinElmer) (1.0 MBq/tube) for 15 min and then resolved in sample buffer (1.0 μl/islet for wild-type and *Eif4ebp1*$^{-/-}$ islets and 0.75 μl/islet for other genotypes). The level of protein synthesis was quantified from autoradiograms. For measurement of *Chop* translation, 4 × 10^6 cells treated with thapsigargin for 12 hr were washed with methionine/cysteine-free DMEM containing 15% dialyzed FCS and labeled with [^{35}S]methionine/cysteine (20 MBq/bottle) for 2 hr. Cells were then resolved in lysis buffer (50 mM Tris [pH 7.5], 150 mM NaCl, 2 mM $MgCl_2$, 0.1% Triton X-100, and protease inhibitors [Roche]). Lysates were precleared with Protein A Sepharose Fast Flow (Amersham) and incubated with anti-CHOP antibody (R-20, Santa Cruz) overnight.

Firefly Luciferase Reporter Assay

Oligonucleotides containing ATF4 binding sites were annealed and subcloned into the pGL3-Promoter vector (BamHI-SalI, Promega). MIN6 cells were transfected with luciferase reporters using Lipofectamine (Invitrogen). Luciferase activity was assayed with a dual-luciferase system (Promega) using a luminometer (Berthold).

Chromatin Immunoprecipitation Assay

Proteins bound to DNA were crosslinked with 1% formaldehyde at 4°C for 20 min. After sonication, the protein-DNA complexes were immunoprecipitated using an anti-ATF4 antibody (C-20, Santa Cruz). After reversal of the crosslinks at 65°C for 6 hr, DNA was purified on a DNA purification column (QIAGEN). PCR was performed with the primers 5′-GATGAGGAAGAGGAAGCTGAGT TG-3′ and 5′-AGTTGTAAGAGGAGTAGTTGGGGG-3′.

Statistical Analysis

Data are presented as means ± SEM. Differences between groups were assessed by Student's t test. $p < 0.05$ was considered significant.

SUPPLEMENTAL DATA

Supplemental Data include six figures and Supplemental References and can be found with this article online at http://www.cellmetabolism.org/cgi/content/full/7/3/269/DC1/.

ACKNOWLEDGMENTS

We thank J. Alam (Alton Ochsner Medical Foundation) and D. Ron (New York University) for their generous gifts of DN-ATF4 cDNA and *Atf4*$^{-/-}$ MEFs, respectively. We are also grateful to K. Igarashi (Tohoku University) for advice on ChIP analysis and to Y. Nagura and K. Tanaka for their expert technical assistance. This work was supported by Grants-in-Aid for Scientific Research

(H) [^{35}S]methionine/cysteine labeling as in (G) in islets of the indicated genotypes at 6–8 weeks of age. Lane 1, wild-type; lane 2, *Eif4ebp1*$^{-/-}$; lane 3, *Wfs1*$^{-/-}$; lane 4, *Eif4ebp1*$^{-/-}$ *Wfs1*$^{-/-}$. Data from three experiments are summarized in the right panel. *$p < 0.05$.
Error bars represent SEM.

(19590300 to H.I. and 19209034 to Y.O.) from the Ministry of Education, Culture, Sports, Science and Technology of Japan.

Received: July 10, 2007
Revised: December 2, 2007
Accepted: January 30, 2008
Published: March 4, 2008

REFERENCES

Butler, A.E., Janson, J., Bonner-Weir, S., Ritzel, R., Rizza, R.A., and Butler, P.C. (2003). β-cell deficit and increased beta-cell apoptosis in humans with type 2 diabetes. Diabetes *52*, 102–110.

Cheyssac, C., Dina, C., Lepretre, F., Vasseur-Delannoy, V., Dechaume, A., Lobbens, S., Balkau, B., Ruiz, J., Charpentier, G., Pattou, F., et al. (2006). EIF4A2 is a positional candidate gene at the 3q27 locus linked to type 2 diabetes in French families. Diabetes *55*, 1171–1176.

Clemens, M.J. (2001). Translational regulation in cell stress and apoptosis. Roles of the eIF4E binding proteins. J. Cell. Mol. Med. *5*, 221–239.

Delepine, M., Nicolino, M., Barrett, T., Golamaully, M., Lathrop, G.M., and Julier, C. (2000). EIF2AK3, encoding translation initiation factor 2-alpha kinase 3, is mutated in patients with Wolcott-Rallison syndrome. Nat. Genet. *25*, 406–409.

Harding, H.P., Novoa, I., Zhang, Y., Zeng, H., Wek, R., Schapira, M., and Ron, D. (2000). Regulated translation initiation controls stress-induced gene expression in mammalian cells. Mol. Cell *6*, 1099–1108.

Harding, H.P., Zeng, H., Zhang, Y., Jungries, R., Chung, P., Plesken, H., Sabatini, D.D., and Ron, D. (2001). Diabetes mellitus and exocrine pancreatic dysfunction in perk−/− mice reveals a role for translational control in secretory cell survival. Mol. Cell *7*, 1153–1163.

Harding, H.P., Zhang, Y., Zeng, H., Novoa, I., Lu, P.D., Calfon, M., Sadri, N., Yun, C., Popko, B., Paules, R., et al. (2003). An integrated stress response regulates amino acid metabolism and resistance to oxidative stress. Mol. Cell *11*, 619–633.

He, C.H., Gong, P., Hu, B., Stewart, D., Choi, M.E., Choi, A.M., and Alam, J. (2001). Identification of activating transcription factor 4 (ATF4) as an Nrf2-interacting protein. Implication for heme oxygenase-1 gene regulation. J. Biol. Chem. *276*, 20858–20865.

Holcik, M., and Sonenberg, N. (2005). Translational control in stress and apoptosis. Nat. Rev. Mol. Cell Biol. *6*, 318–327.

Ibrahimo, S., Holmes, L.E., and Ashe, M.P. (2006). Regulation of translation initiation by the yeast eIF4E binding proteins is required for the pseudohyphal response. Yeast *23*, 1075–1088.

Inoue, H., Tanizawa, Y., Wasson, J., Behn, P., Kalidas, K., Bernal-Mizrachi, E., Mueckler, M., Marshall, H., Donis-Keller, H., Crock, P., et al. (1998). A gene encoding a transmembrane protein is mutated in patients with diabetes mellitus and optic atrophy (Wolfram syndrome). Nat. Genet. *20*, 143–148.

Ishihara, H., Takeda, S., Tamura, A., Takahashi, R., Yamaguchi, S., Takei, D., Yamada, T., Inoue, H., Soga, H., Katagiri, H., et al. (2004). Disruption of the WFS1 gene in mice causes progressive beta-cell loss and impaired stimulus-secretion coupling in insulin secretion. Hum. Mol. Genet. *13*, 1159–1170.

Koritzinsky, M., Magagnin, M.G., van den Beucken, T., Seigneuric, R., Savelkouls, K., Dostie, J., Pyronnet, S., Kaufman, R.J., Weppler, S.A., Voncken, J.W., et al. (2006). Gene expression during acute and prolonged hypoxia is regulated by distinct mechanisms of translational control. EMBO J. *25*, 1114–1125.

Laybutt, D.R., Preston, A.M., Akerfeldt, M.C., Kench, J.G., Busch, A.K., Biankin, A.V., and Biden, T.J. (2007). Endoplasmic reticulum stress contributes to beta cell apoptosis in type 2 diabetes. Diabetologia *50*, 752–763.

Miyazaki, J., Araki, K., Yamato, E., Ikegami, H., Asano, T., Shibasaki, Y., Oka, Y., and Yamamura, K. (1990). Establishment of a pancreatic beta cell line that retains glucose-inducible insulin secretion: special reference to expression of glucose transporter isoforms. Endocrinology *127*, 126–132.

Novoa, I., and Carrasco, L. (1999). Cleavage of eukaryotic translation initiation factor 4G by exogenously added hybrid proteins containing poliovirus 2Apro in HeLa cells: effects on gene expression. Mol. Cell. Biol. *19*, 2445–2454.

Novoa, I., Zeng, H., Harding, H.P., and Ron, D. (2001). Feedback inhibition of the unfolded protein response by GADD34-mediated dephosphorylation of eIF2α. J. Cell Biol. *153*, 1011–1022.

Pirot, P., Naamane, N., Libert, F., Magnusson, N.E., Orntoft, T.F., Cardozo, A.K., and Eizirik, D.L. (2007). Global profiling of genes modified by endoplasmic reticulum stress in pancreatic beta cells reveals the early degradation of insulin mRNAs. Diabetologia *50*, 1006–1014.

Riggs, A.C., Bernal-Mizrachi, E., Ohsugi, M., Wasson, J., Fatrai, S., Welling, C., Murray, J., Schmidt, R.E., Herrera, P.L., and Permutt, M.A. (2005). Mice conditionally lacking the Wolfram gene in pancreatic islet beta cells exhibit diabetes as a result of enhanced endoplasmic reticulum stress and apoptosis. Diabetologia *48*, 2313–2321.

Rutkowski, D.T., Arnold, S.M., Miller, C.N., Wu, J., Li, J., Gunnison, K.M., Mori, K., Sadighi Akha, A.A., Raden, D., and Kaufman, R.J. (2006). Adaptation to ER stress is mediated by differential stabilities of pro-survival and pro-apoptotic mRNAs and proteins. PLoS Biol. *4*, e374.

Scheuner, D., Mierde, D.V., Song, B., Flamez, D., Creemers, J.W., Tsukamoto, K., Ribick, M., Schuit, F.C., and Kaufman, R.J. (2005). Control of mRNA translation preserves endoplasmic reticulum function in β cells and maintains glucose homeostasis. Nat. Med. *11*, 757–764.

Schroder, M., and Kaufman, R.J. (2005). The mammalian unfolded protein response. Annu. Rev. Biochem. *74*, 739–789.

Strom, T.M., Hortnagel, K., Hofmann, S., Gekeler, F., Scharfe, C., Rabl, W., Gerbitz, K.D., and Meitinger, T. (1998). Diabetes insipidus, diabetes mellitus, optic atrophy and deafness (DIDMOAD) caused by mutations in a novel gene (wolframin) coding for a predicted transmembrane protein. Hum. Mol. Genet. *7*, 2021–2028.

Teleman, A.A., Chen, Y.W., and Cohen, S.M. (2005). 4E-BP functions as a metabolic brake used under stress conditions but not during normal growth. Genes Dev. *19*, 1844–1848.

Tettweiler, G., Miron, M., Jenkins, M., Sonenberg, N., and Lasko, P.F. (2005). Starvation and oxidative stress resistance in Drosophila are mediated through the eIF4E-binding protein, d4E-BP. Genes Dev. *19*, 1840–1843.

Tsukiyama-Kohara, K., Poulin, F., Kohara, M., DeMaria, C.T., Cheng, A., Wu, Z., Gingras, A.C., Katsume, A., Elchebly, M., Spiegelman, B.M., et al. (2001). Adipose tissue reduction in mice lacking the translational inhibitor 4E-BP1. Nat. Med. *7*, 1128–1132.

Wang, J., Takeuchi, T., Tanaka, S., Kubo, S.K., Kayo, T., Lu, D., Takata, K., Koizumi, A., and Izumi, T. (1999). A mutation in the insulin 2 gene induces diabetes with severe pancreatic β-cell dysfunction in the Mody mouse. J. Clin. Invest. *103*, 27–37.

Zhang, P., McGrath, B., Li, S., Frank, A., Zambito, F., Reinert, J., Gannon, M., Ma, K., McNaughton, K., and Cavener, D.R. (2002). The PERK eukaryotic initiation factor 2α kinase is required for the development of the skeletal system, postnatal growth, and the function and viability of the pancreas. Mol. Cell. Biol. *22*, 3864–3874.

Cell Metabolism, Volume 7

Supplemental Data

Short Article

ATF4-Mediated Induction of 4E-BP1 Contributes to Pancreatic β Cell Survival under Endoplasmic Reticulum Stress

Suguru Yamaguchi, Hisamitsu Ishihara, Takahiro Yamada, Akira Tamura, Masahiro Usui, Ryu Tominaga, Yuichiro Munakata, Chihiro Satake, Hideki Katagiri, Fumi Tashiro, Hiroyuki Aburatani, Kyoko Tsukiyama-Kohara, Jun-ichi Miyazaki, Nahum Sonenberg, and Yoshitomo Oka

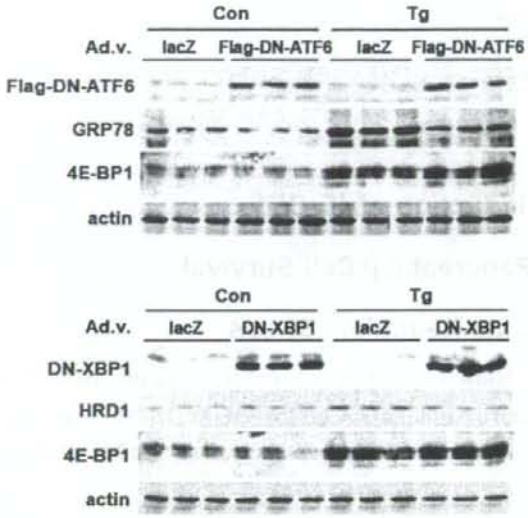

Figure S1. Effects of DN-ATF or DN-XBP1 Expression on 4E-BP1 Induction

Upper panel: no suppression of thapsigargin-triggered 4E-BP1 induction with expression of the Flag-tagged dominant-negative (DN) ATF6 (Flag-DN-ATF6: ATF6(171-373) lacking the activation domain (Yoshida et al., 2000)). MIN6 cells infected with an adenovirus expressing either lacZ or the Flag-DN-ATF6 were treated with vehicle (0.05% DMSO) control (Con) or thapsigargin (Tg, 0.5 μM) for 12 hr. Cell lysates were analyzed for expressions of Flag-DN-ATF6, GRP78 (ATF6-target), 4E-BP1 and actin (loading control).

Lower panel: no suppression of Tg-triggered 4E-BP1 induction with expression of the DN-XBP1 (XBP1(1-188) lacking the activation domain (Lee et al., 2003)). MIN6 cells infected with an adenovirus expressing either lacZ or the DN-XBP1 were treated with vehicle control (Con) or Tg for 12 hr. Cell lysates were analyzed for expressions of DN-XBP1, HRD1 (XBP1-target), 4E-BP1 and actin (loading control).

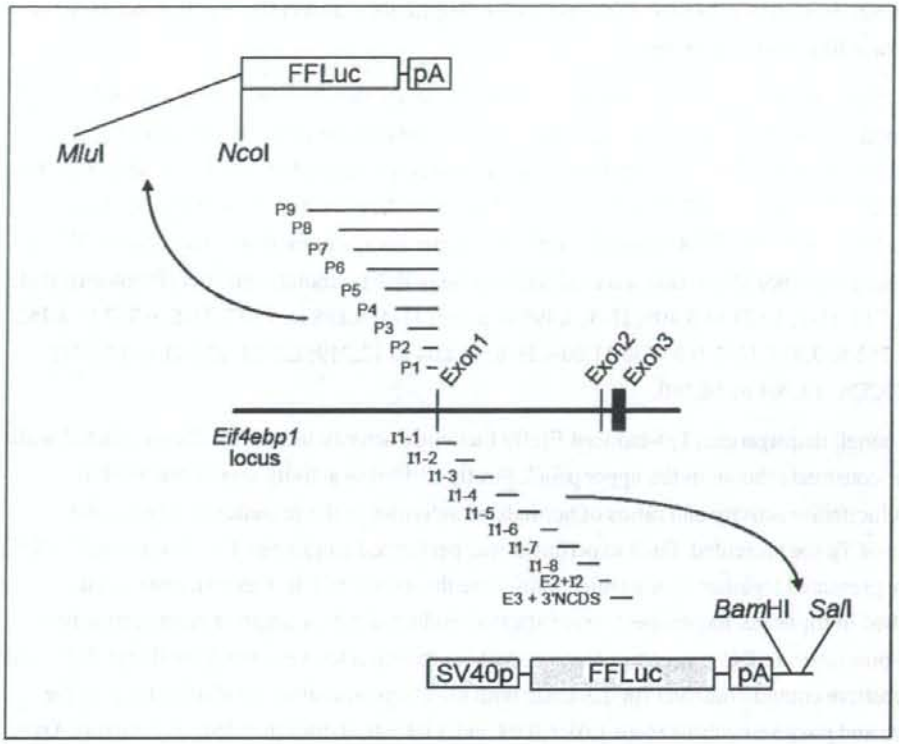
FFLuc
pA
MluI
NcoI
P9
P8
P7
P6
P5
P4
P3
P2
P1
Exon1
Exon2
Exon3
Eif4ebp1
locus
I1-1
I1-2
I1-3
I1-4
I1-5
I1-6
I1-7
I1-8
E2+I2
E3 + 3'NCDS
BamHI
SalI
SV40p
FFLuc
pA

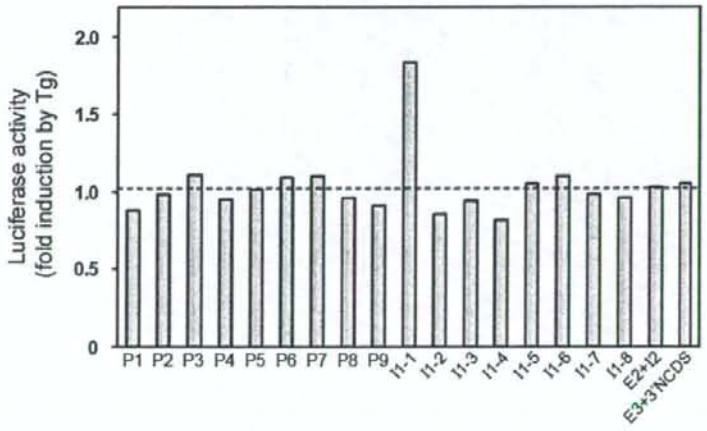
Luciferase activity
(fold induction by Tg)
2.0
1.5
1.0
0.5
0
P1 P2 P3 P4 P5 P6 P7 P8 P9 I1-1 I1-2 I1-3 I1-4 I1-5 I1-6 I1-7 I1-8 E2+I2 E3+3'NCDS

Figure S2. Search for Mouse *Eif4ebp1* Gene Segments Conferring Tg Responsiveness to Luciferase Reporter Constructs

Upper panel: reporter constructs used for luciferase activity measurements are presented. PCR-amplified *Eif4ebp1* promoter segments were cloned into the pGL3-basic construct (Promega). P1, -1 to –260 (A in the initial ATG codon is determined as +1); P2, -1 to -1,129; P3, -1 to -2,216; P4, -1 to -3,182; P5, -1 to –4,027; P6, -1 to -4,791; P7, -1 to –6,537; P8, -1 to -7,978; P9, -1 to -9,968. PCR-amplified *Eif4ebp1* segments spanning from exon 1 to the 3' non-coding sequence (3'NCDS) were cloned into the pGL3-promoter construct (Promega). I1-1, +1 to 1,821; I1-2, 1,821 to 3,409; I1-3, 3,409 to 5,198; I1-4, 5,198 to 6,957; I1-5, 6,957 to 8,752; I1-6, 8,752 to 9,977; I1-7, 9,977 to 11,804; I1-8, 11,804 to 12,949; E2+I2, 12,921 to 14,703; E3+3'NCDS, 14,704 to 16,260.

Lower panel: thapsigargin (Tg)-induced firefly luciferase activity in MIN6 cells transfected with reporter constructs shown in the upper panel. Firefly luciferase activity was normalized to Renilla luciferase activity and ratios of normalized activities in the presence to those in the absence of Tg are presented. Each experiment was performed employing 1 or 2 constructs and all data are presented together in one panel. Values are the means of 1 to 3 experiments, each performed in triplicate. Experiments were always conducted with a negative control construct (pGL3-promoter: a *SV40* promoter construct with no insertion between the *Bam*HI and *Sal*I sites) and a positive control construct (pGL3-basic with the *Chop* promoter). Fold inductions of the negative and positive controls were 1.03 ± 0.09 and 3.04 ± 0.11-fold (n = 25), respectively. Data obtained with the negative control are shown as a dashed line.

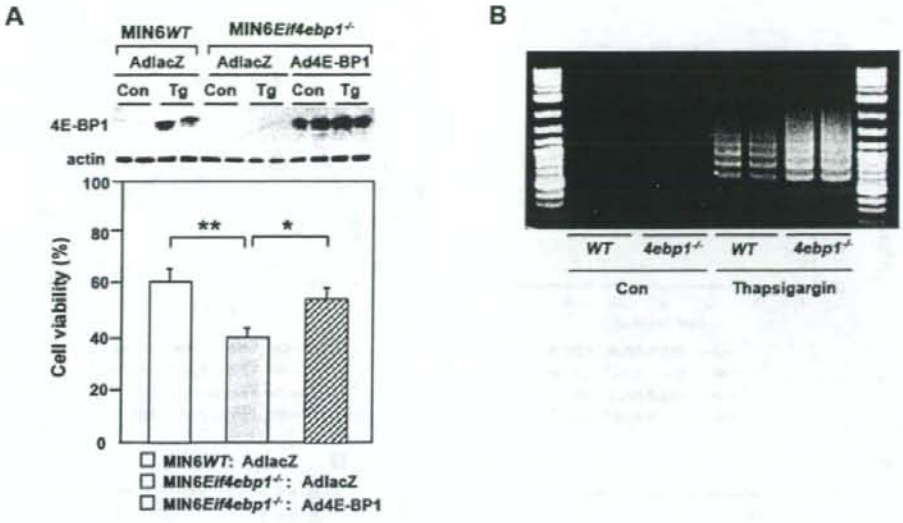

Figure S3. Higher Sensitivity of 4E-BP1-Deficient MIN6 Cells and Islets to ER Stress

(A) Reduced viability of MIN6*Eif4ebp1*$^{-/-}$ cells treated with 0.5 μM thapsigargin (Tg) was restored by re-expression of 4E-BP1. Data from MIN6*WT* cells treated with vehicle (0.05% DMSO) were taken as 100%. Error bars show SEM. n = 4; *p < 0.05, **p < 0.01. Adenovirus-mediated re-expression of 4E-BP1 is shown in the upper panel. Con, vehicle-treated cells.

(B) Increased apoptotic DNA ladder formation in isolated islets from *Eif4ebp1*$^{-/-}$ mice. Islets isolated from mice of each genotype at 12 weeks of age were incubated in RPMI medium for 3 days and DNA fragmentation was analyzed by ligation-mediated PCR as described previously (Ishihara et al., 2004).

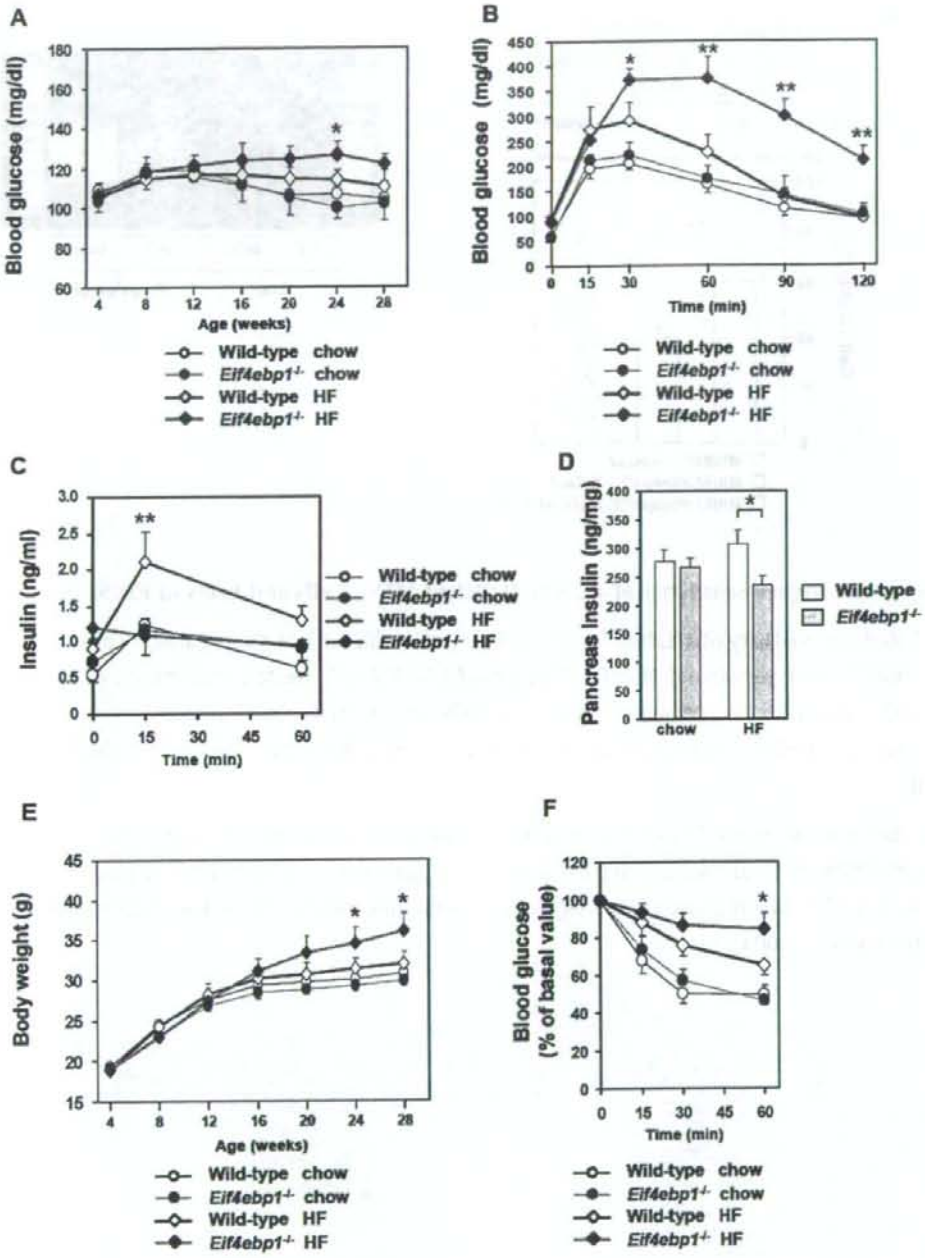
A
Blood glucose (mg/dl)
Age (weeks)
Wild-type chow
Eif4ebp1-/- chow
Wild-type HF
Eif4ebp1-/- HF
B
Blood glucose (mg/dl)
Time (min)
C
Insulin (ng/ml)
Time (min)
D
Pancreas Insulin (ng/mg)
chow
HF
Wild-type
Eif4ebp1-/-
E
Body weight (g)
Age (weeks)
F
Blood glucose (% of basal value)
Time (min)